

# Experimental aspects of quarkonia production and suppression in cold and hot nuclear matter

ANTHONY D FRAWLEY<sup>1</sup>

*Department of Physics  
Florida State University, Tallahassee, FL 32306, USA*

When heavy Quarkonia are formed in collisions between nuclei, their production cross section is modified relative to that in  $p + p$  collisions. The physical effects that cause this modification fall into two categories. Hot matter effects are due to the large energy density generated in the nuclear collision, which disrupts the formation of the quarkonium state. Cold nuclear matter effects are due to the fact that the quarkonium state is created in a nuclear target. I will review experimental aspects of quarkonia production due to both hot and cold matter effects.

PRESENTED AT

The 7th International Workshop on Charm Physics  
(CHARM 2015)  
Detroit, MI, 18-22 May, 2015

---

<sup>1</sup>Work supported by NSF award no. 106489.

# 1 Introduction

Interest in studying quarkonia production in high energy heavy ion collisions was motivated decades ago by the prediction that  $J/\psi$  formation would be suppressed by color screening effects in the Quark Gluon Plasma (QGP) [1]. But experience has shown that relating  $J/\psi$  suppression to the energy densities of the hot matter formed in heavy ion collisions is complicated by the presence of competing effects that also modify  $J/\psi$  production. The importance of this is illustrated in Figure 1 where the nuclear modification factor,  $R_{AA}$ , is plotted versus collision centrality for collisions of heavy nuclei at  $\sqrt{s_{NN}} = 17.3$  to 200 GeV. There is no obvious dependence on the energy density produced in the collision. The measured nuclear modification factors are similar at mid rapidity at the two widely different collision energies, but at 200 GeV show more suppression at forward rapidity, where the energy density is slightly smaller than at mid rapidity. Interpreting the data requires a detailed understanding of the mechanisms that compete with color screening.

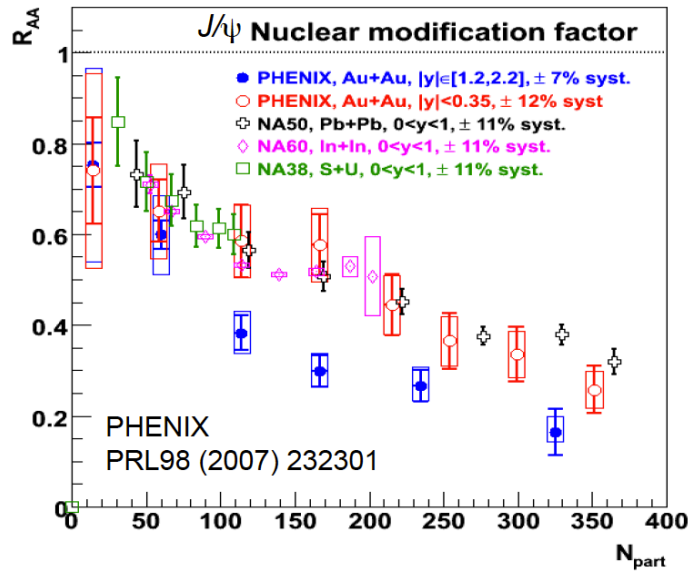


Figure 1: The nuclear modification factor versus collision centrality for collisions of heavy nuclei at energies of  $\sqrt{s_{NN}} = 17.3$  (In+In, Pb+Pb), 19.4 GeV (S+U), and 200 GeV (Au+Au).

In general, quarkonia production is modified by both cold nuclear matter (CNM) effects and hot matter effects [2] CNM effects modify the yield or kinematic distributions of  $J/\psi$  produced in a nuclear target in the absence of a QGP. They include modification of parton densities in a nucleus [3, 4, 5, 6, 7], breakup of the charmonium or bottomonium or its precursor  $Q\bar{Q}$  state in the nuclear target due to collisions with nucleons [8, 9, 10], transverse momentum broadening as the  $Q\bar{Q}$  traverses the

cold nucleus, and initial state parton energy loss [11]. CNM effects are expected to be strongly dependent on collision system, collision energy, rapidity and collision centrality.

In hot matter, there is not only suppression of quarkonia yields by color screening effects that reduce the binding energy of the quarkonium state, but also enhancement of quarkonia yields due to coalescence of  $Q\bar{Q}$  pairs that are initially unbound, but which become bound due to interactions with the medium (see for example [12]). In particular, at LHC collision energies the yield of  $J/\psi$  from coalescence of a  $c$  and  $\bar{c}$  from different hard processes becomes dominant.

When discussing modification of quarkonia yields in nuclear collisions, the hierarchy of relevant time scales is very important. The nuclear crossing time for Lorentz contracted nuclei at RHIC(LHC) energies is  $\sim 0.3(0.001)$  fm/ $c$ . The formation time of a  $J/\psi$  meson in its rest frame is  $\sim 0.3$  fm/ $c$ . The QGP thermalization time is  $\sim 0.3 - 0.6$  fm/ $c$ . The QGP lifetime in central collisions at RHIC energy is  $\sim 5 - 7$  fm/ $c$ , longer at LHC energies. The  $J/\psi$  lifetime is  $\sim 2000$  fm/ $c$ . Thus the creation of quarkonia and their modification in the hot medium occur on different time scales. They are often taken as factorable, although there are some theoretical models in which they can not be factorized [13].

## 2 proton-Nucleus collisions as a reference for CNM effects

CNM effects are observed in either  $p+A$  or  $d+A$  collisions, which allow us to study the modification of quarkonia yields when they are produced in a nuclear target. It should be noted here that  $p+A$  collisions involving heavy targets appear to produce a small hot spot containing a large energy density, as evidenced by the observation of collective flow effects [14]. However when studying hard probes (jets or heavy quarkonia),  $p+A$  collisions differ from  $A+A$  collisions. In  $p+A$  collisions the hot matter and the hard probes are both produced in a transverse area defined by the radius of the projectile proton. In  $A+A$  collisions however a high energy density is produced throughout the collision volume, and the hard probe is typically immersed in that extended volume of evolving hot matter for several fm/ $c$  or more. We will return later to the question of whether the small hot spot produced in  $p+A$  collisions significantly modifies the yield of hard probes.

There have been several studies of  $p+A$  or  $d+A$  data in which  $p_T$  integrated  $J/\psi$   $R_{AA}$  values were corrected for shadowing effects using a shadowing parameterization, and then the data were fitted to extract an effective absorption cross section,  $\sigma_{abs}$ , where  $\sigma_{abs}$  accounts for all effects that modify  $J/\psi$  production aside from shadowing. If it is assumed that CNM effects can be factorized from hot matter effects, then heavy ion collision data can be corrected for CNM effects using this parameterization

of the  $p+A$  data.

In one such study (see section 5 of [2])  $d+Au$   $R_{CP}$  data from PHENIX at  $\sqrt{s_{NN}} = 200$  GeV were corrected for shadowing effects using the EPS09 parameterization and values of  $\sigma_{abs}$  extracted at rapidities of  $-2.2 < y < -1.2$ ,  $y < 0.35$  and  $1.2 < y < 2.2$ . The parametrization was then used in a Glauber model to estimate the contribution to the Au+Au  $R_{AA}$  from CNM effects at  $y < 0.35$  and  $1.2 < |y| < 2.2$ , and the measured Au+Au  $R_{AA}$  was divided by the CNM  $R_{AA}$ . The result is shown in Figure 2 (left). Comparison with Fig. 1 shows that the correction for CNM effects eliminates the large difference in suppression for the Au+Au data at mid and forward rapidity.

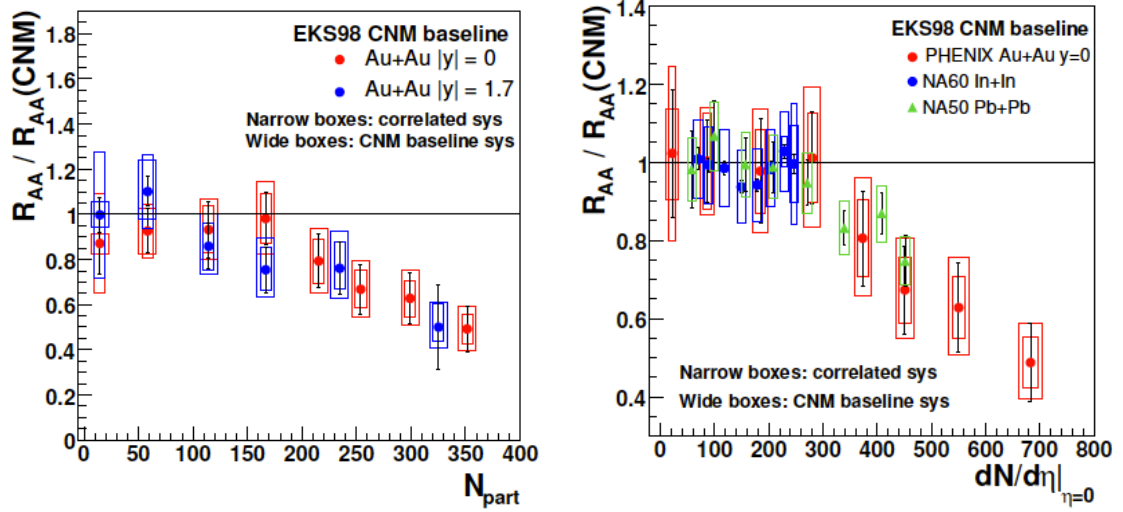


Figure 2: Left: The measured  $R_{AA}$  for  $J/\psi$  production at 200 GeV at  $y = 0$  and  $y = 1.7$  divided by the estimated  $R_{AA}$  due to CNM effects. Right: Comparison of the measured  $R_{AA}$  divided by the estimated  $R_{AA}$  due to CNM effects for  $J/\psi$  production in Pb+Pb collisions at  $\sqrt{s_{NN}} = 17.3$  GeV at  $y = 0.5$  and in Au+Au collisions at  $\sqrt{s_{NN}} = 200$  GeV at  $y = 0$

In a similar study of  $p+Pb$  data from the NA60 experiment at  $\sqrt{s_{NN}} = 17.3$  GeV, the  $R_{AA}$  was corrected for shadowing effects using the EKS98 parameterization, and then the value of  $\sigma_{abs}$  extracted [9]. This was used to estimate the contribution to the  $R_{AA}$  in Pb+Pb collisions so that the measured Pb+Pb  $R_{AA}$  could be corrected for CNM effects. In Figure 2 (right) the resulting CNM corrected results at  $\sqrt{s_{NN}} = 17.3$  GeV and  $y = 0.5$  are compared with the CNM corrected mid rapidity data for Au+Au at  $\sqrt{s_{NN}} = 200$  GeV. The data are presented as a function of  $dN/d\eta$ , which is used as a proxy for energy density. It is found that when the A+A data are corrected for CNM effects the remaining nuclear modification seems to scale with energy density, and is about 50% for central collisions at RHIC energy.

### 3 Nucleus-Nucleus collisions and coalescence

As mentioned earlier, in addition to suppression of the quarkonia due to color screening, there is another effect that can occur due to QGP formation - coalescence. There are two coalescence scenarios.

In the first, a  $Q$  and  $\bar{Q}$  that were produced in the same hard process, and are nearly bound, can become bound through interactions with the medium. This first scenario occurs even if only one heavy quark pair is produced in a collision, and is present to some degree at all collision energies. It is sometimes referred to as "regeneration".

In the second scenario, a  $Q$  and  $\bar{Q}$  that were produced in different hard processes can thermalize in the medium and combine statistically at hadronization. This second scenario becomes important only if a single collision produces many heavy quark pairs. At LHC energies we expect that  $\sim 100$   $c\bar{c}$  pairs are created in a central Pb+Pb collision.

Figure 3 shows a comparison of measured  $R_{AA}$  values for  $\sqrt{s_{NN}} = 2.76$  TeV ALICE Pb+Pb results and  $\sqrt{s_{NN}} = 200$  GeV PHENIX Au+Au results. The data, measured at forward rapidity in both cases, are plotted versus  $dN_{ch}/d\eta$ , which is used as a proxy for energy density. The suppression for the lower energy data is far stronger than for the higher energy data, suggesting that coalescence is now dominant. Indeed, the increase in  $J/\psi$  yield at the higher energy is concentrated at lower transverse momentum, as predicted by models that include coalescence at LHC energies [15].

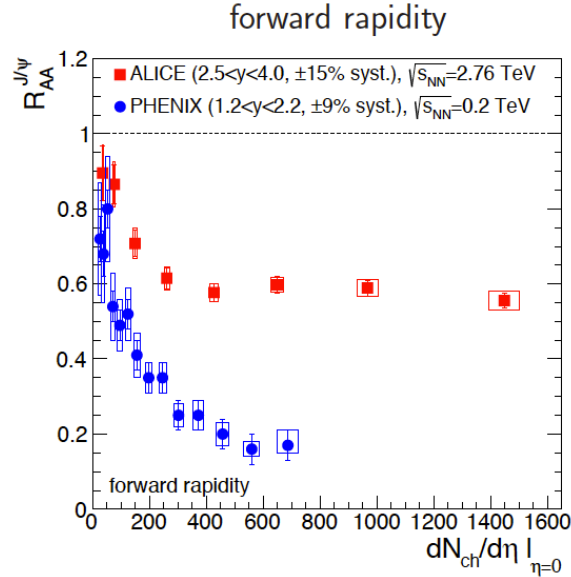


Figure 3: Comparison of  $J/\psi$   $R_{AA}$  data at  $\sqrt{s_{NN}} = 2.76$  TeV by ALICE with  $J/\psi$   $R_{AA}$  data by PHENIX at 200 GeV.

Of the A+A data available so far, the strongest suppression occurs at RHIC energy, presumably because at the higher LHC energies the gain in  $J/\psi$  yield overcomes the loss due to stronger color screening effects. It is interesting to look at the dependence of the suppression for Au+Au on collision energy. Figure 4 shows  $R_{AA}$  vs centrality for Au+Au collisions at  $\sqrt{s_{NN}} = 39, 62$  and 200 GeV [16]. The data are compared with theoretical calculations that include coalescence [12]. The measured  $R_{AA}$  is found to be similar at all three energies, and in the calculations that similarity is expected as a result of the stronger suppression due to color screening being balanced by an increased coalescence component as the energy increases.

In addition to the Au+Au data, there are preliminary U+U  $J/\psi$  data at  $\sqrt{s_{NN}} = 193$  GeV from PHENIX at forward rapidity. They show slightly weaker suppression for central collisions than is seen in Au+Au data. This is consistent with a picture in which the increased suppression from the higher energy density in the U+U collision is more than balanced by the increased charm production from the larger number of nucleon-nucleon collisions in U+U [17].

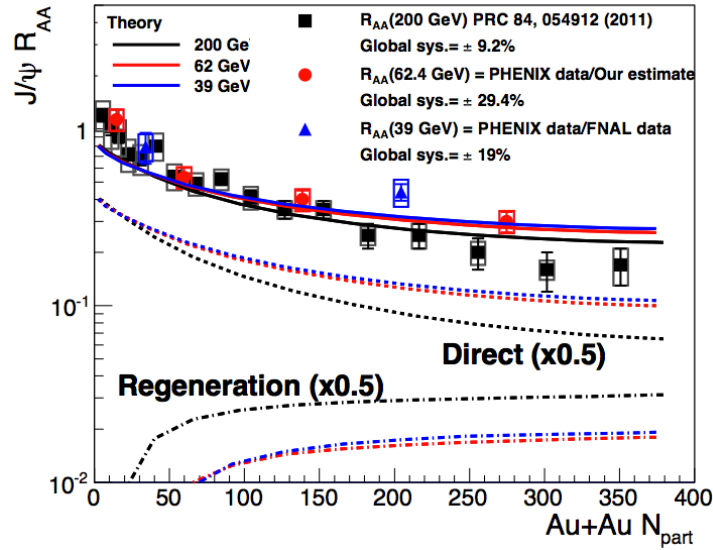


Figure 4: The  $R_{AA}$  for Au+Au collisions at  $\sqrt{s_{NN}} = 39, 62$  and 200 GeV from PHENIX, compared with calculations that include both suppression due to color screening and coalescence.

## 4 CNM effects in proton-Nucleus collisions

There was a comprehensive study of fixed target  $J/\psi$   $p$ +A data from five fixed target experiments [8] in which the measured  $R_{AA}$  values for centrality integrated data were

corrected for shadowing effects using the EKS98 parameterization, and then fitted with an effective absorption cross section. Additionally there is a value of  $\sigma_{abs}$  for the  $J/\psi$  from EKS98 corrected  $p$ +Pb data at  $\sqrt{s_{NN}} = 17.3$  GeV from [9]. A similar study of  $J/\psi$   $R_{AA}$  values from  $\sqrt{s_{NN}} = 200$  GeV  $d$ +Au collisions at nine rapidities, this time corrected for shadowing using the EPS09 parameterization, was made in [10]. The  $\sigma_{abs}$  values extracted from all seven data sets were plotted versus the nuclear crossing time - the proper time in the rest frame of the evolving charmonium state during which it is exposed to collisions with nuclei. The results from [10] are presented in Figure 5.

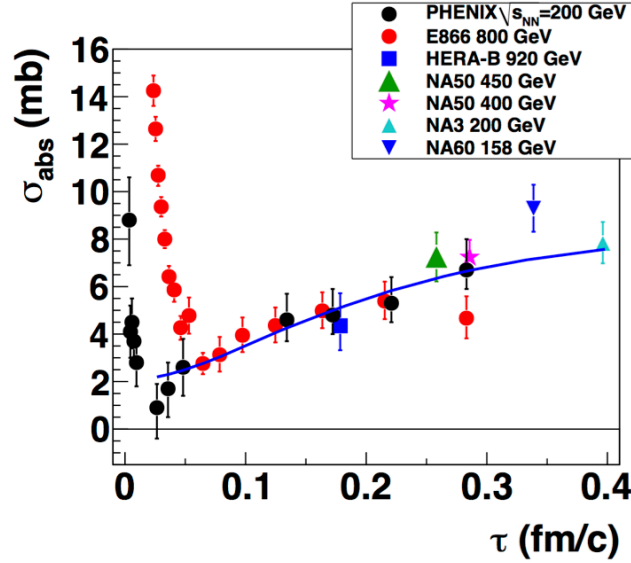


Figure 5: Effective absorption cross sections extracted from shadowing corrected  $p$ +A or  $d$ +A data at a range of collision energies from  $\sqrt{s_{NN}} = 17.3$  to 200 GeV, plotted versus proper time spent in the target nucleus by the evolving charmonium state. The curve is discussed in the text.

For nuclear crossing times of  $\tau > 0.05$   $fm/c$  the data at different energies seem to scale well with  $\tau$ . The data at  $\tau > 0.05 fm/c$  were fitted [10] with a model of an expanding color neutral meson passing through the target [18], showing that the data in this  $\tau$  range are consistent with breakup of charmonia. For shorter nuclear crossing times no such scaling is observed. This is expected, since those nuclear crossing times are shorter than the  $c\bar{c}$  formation time, suggesting that for short nuclear crossing times the effective absorption cross section reflects physical processes other than breakup of the charmonia, such as energy loss in cold nuclear matter.

The observation of elliptic flow in  $p$ +A collisions at LHC energies and  $d$ +A collisions at RHIC energies (see for example [14]) suggests that a small fireball is produced

in those collisions. This raises the question of whether quarkonia production in  $p+A$  collisions is modified by final state effects.

For the  $J/\psi$ , the  $p+A$  data from ALICE at the LHC seem to be consistent with models of CNM effects, including coherent energy loss at forward rapidity [15], although there are significant experimental and theoretical uncertainties. At RHIC energy, with similar caveats, there is no strong evidence that more than CNM effects are needed to describe the PHENIX  $d+Au$   $J/\psi$  data [19]. It is worth noting also that the scaling observed with  $\tau$  in Fig. 5 for  $\tau > 0.5$   $fm/c$  would be broken if there were strong final state effects in  $d+Au$  collisions at 200 GeV, but it seems to hold within the uncertainties on the extracted  $\sigma_{abs}$  values. In all cases, however, because feed down from the  $\psi'$  accounts for only about 10% of the inclusive  $J/\psi$  yield, it is still possible that the very weakly bound  $\psi'$  is significantly modified by final state effects.

Unexpectedly strong suppression of  $\psi'$  yields in central  $d+Au$  collisions was observed at  $\sqrt{s_{NN}} = 200$  GeV at mid rapidity by PHENIX [20], as shown in Figure 6. A very similar strong suppression of the  $\psi'$  yield is observed in central  $p+Pb$  collisions at  $\sqrt{s_{NN}} = 2.76$  TeV at both forward and backward rapidity in ALICE preliminary data [21]. The strong differential suppression of the  $\psi'$  relative to the  $J/\psi$  can not be due to a larger nucleon breakup cross section for the larger, more weakly bound  $\psi'$  because the nuclear crossing time is too short at all of the collision energies and rapidities of the data. Nor is it expected from any other known CNM process. It seems likely that the strong  $\psi'$  suppression is caused by final state effects. Destruction of the  $\psi'$  by co-moving particles in the final state has been proposed as an explanation [22].

## 5 Upsilon

The comparison of charmonium measurements at RHIC and LHC energies has revealed some very interesting physics. However it has not provided a direct comparison of color screening effects at RHIC and LHC temperatures because the dominant mechanism for charmonium production at LHC energies, charm coalescence, is different from that at RHIC energies, where color screening dominates.

The study of Upsilon production in A+A collisions offers several advantages over charmonium. First, the  $\Upsilon(1S)$ ,  $\Upsilon(2S)$  and  $\Upsilon(3S)$  states all have significant branches to dileptons, and can thus be observed in the same experiment. The three states span a broad range of binding energies and sizes, and have similar shadowing effects. Importantly, the  $\Upsilon$  states will not have large coalescence contributions at RHIC or LHC because the bottom production rate in central collisions at LHC energies is similar to the charm pair production rate at RHIC. On the down side, the  $\Upsilon$  production cross sections are small, and the difference in mass between the states is also small. Therefore mass resolved  $\Upsilon$  measurements require large luminosity, large detector acceptance, and excellent momentum resolution.



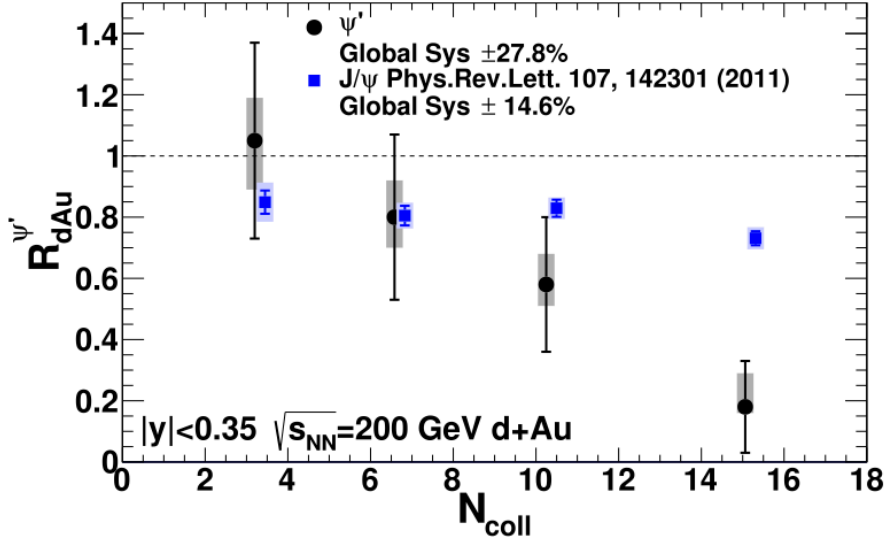


Figure 6: The  $R_{dAu}$  for  $\psi'$  production in  $d+Au$  collisions at  $\sqrt{s_{NN}} = 200$  GeV measured at mid rapidity by PHENIX. The  $R_{dAu}$  for  $J/\psi$  production is shown for comparison.

CMS has measured the ratios of  $\Upsilon(2S)$  and  $\Upsilon(3S)$  to  $\Upsilon(1S)$  in  $p+p$  and  $p+Pb$  collisions [23]. In  $p+Pb$  collisions they observe that the  $\Upsilon(2S)$  and  $\Upsilon(3S)$  are differentially suppressed relative to the  $\Upsilon(1S)$  by about 17% and 30% respectively. The differential suppression of the excited states is found to be stronger for events with larger particle production, suggesting that the larger number of particles in the final state has a stronger effect on the more weakly bound states.

The CMS experiment has measured the  $\Upsilon$  modification in  $Pb+Pb$  collisions at  $\sqrt{s_{NN}} = 2.76$  GeV [24]. The  $R_{AA}$  values are shown in Figure 7 for the  $\Upsilon(1S)$  and  $\Upsilon(2S)$  states. The  $\Upsilon(3S)$  state is so strongly suppressed that values were not extracted. The fact that the (2S) and (3S) states are much more strongly suppressed than the (1S) state is suggestive of stronger color screening suppression for the larger, more weakly bound excited states. The data are well described by models in which an  $\Upsilon$  potential model is modified by color screening in an evolving quark gluon plasma [25, 26]. The statistical precision of the LHC data is expected to improve greatly during future planned running of the LHC program.

The measurement of Upsilon at RHIC energy is very challenging because the production cross sections are small. So far, the measurements have been made with low statistical precision. The three states are unresolved in PHENIX, while in STAR only the  $\Upsilon(1S)$  state can be separated by line-shape fitting. Therefore the existing RHIC measurements [27, 28] do not provide strong constraints on theoretical models. This will change in the future with data from the new STAR MTD detector [29],

which was operational in the 2014 RHIC run, and future data from the proposed sPHENIX experiment at RHIC [30].

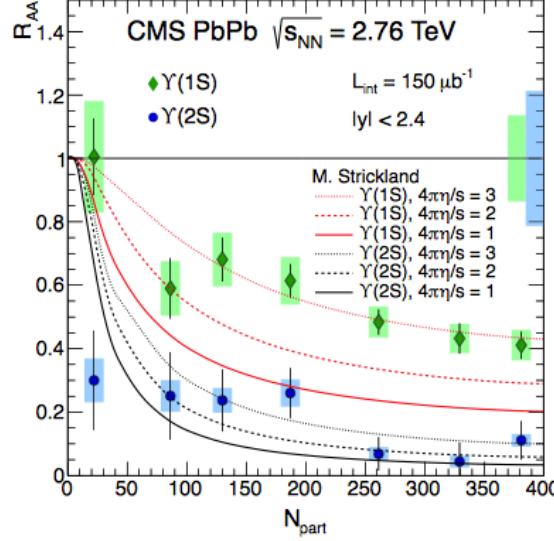


Figure 7: The  $R_{pPb}$  for  $\Upsilon$  production at  $\sqrt{s_{NN}} = 2.76$  TeV measured at mid rapidity by CMS. The theory curves are from [26].

## References

- [1] T. Matsui and H. Satz, Phys. Lett. B **178**, 416 (1986).
- [2] N. Brambilla *et al.*, Eur. Phys. J. C **71**, 1534 (2011)
- [3] M. Hirai, S. Kumano and T.-H. Nagai, Phys. Rev. C **76**, 065207 (2007)
- [4] K. J. Eskola, H. Paukkunen and C. A. Salgado, JHEP **0904**, 065 (2009)
- [5] K. Kovarik, I. Schienbein, F. I. Olness, J. Y. Yu, C. Keppel, J. G. Morfin, J. F. Owens and T. Stavreva, Phys. Rev. Lett. **106**, 122301 (2011)
- [6] D. de Florian, R. Sassot, P. Zurita and M. Stratmann, Phys. Rev. D **85**, 074028 (2012)
- [7] I. Helenius, K. J. Eskola, H. Honkanen and C. A. Salgado, JHEP **1207**, 073 (2012)
- [8] C. Lourenco, R. Vogt and H. K. Woehri, JHEP **0902**, 014 (2009)

- [9] R. Arnaldi *et al.* [NA60 Collaboration], Phys. Lett. B **706**, 263 (2012)
- [10] D. C. McGlinchey, A. D. Frawley and R. Vogt, Phys. Rev. C **87**, 054910 (2013)
- [11] F. Arleo and S. Peigne, Phys. Rev. Lett. **109**, 122301 (2012)
- [12] X. Zhao and R. Rapp, Phys. Rev. C **82**, 064905 (2010)
- [13] B. Z. Kopeliovich, I. K. Potashnikova, H. J. Pirner and I. Schmidt, Phys. Rev. C **83**, 014912 (2011)
- [14] V. Khachatryan *et al.* [CMS Collaboration], Phys. Rev. Lett. **115**, 012301 (2015)
- [15] J. Adam *et al.* [ALICE Collaboration], arXiv:1506.08808 [nucl-ex].
- [16] A. Adare *et al.* [PHENIX Collaboration], Phys. Rev. C **86**, 064901 (2012)
- [17] D. Kikola, G. Odyniec and R. Vogt, Phys. Rev. C **84**, 054907 (2011)
- [18] F. Arleo, P. B. Gossiaux, T. Gousset and J. Aichelin, Phys. Rev. C **61**, 054906 (2000)
- [19] A. Adare *et al.* [PHENIX Collaboration], Phys. Rev. C **87**, 034904 (2013)
- [20] A. Adare *et al.* [PHENIX Collaboration], Phys. Rev. Lett. **111**, 202301 (2013)
- [21] R. Arnaldi [ALICE Collaboration], Nucl. Phys. A **931**, 628 (2014)
- [22] E. G. Ferreira, Phys. Lett. B **749**, 98 (2015)
- [23] S. Chatrchyan *et al.* [CMS Collaboration], JHEP **1404**, 103 (2014)
- [24] S. Chatrchyan *et al.* [CMS Collaboration], Phys. Rev. Lett. **109**, 222301 (2012)
- [25] A. Emerick, X. Zhao and R. Rapp, Eur. Phys. J. A **48**, 72 (2012)
- [26] M. Strickland and D. Bazow, Nucl. Phys. A **879**, 25 (2012)
- [27] A. Adare *et al.* [PHENIX Collaboration], Phys. Rev. C **91**, 024913 (2015)
- [28] R. Vertesi [for the STAR Collaboration], arXiv:1509.05359 [hep-ex].
- [29] L. Ruan *et al.*, J. Phys. G **36**, 095001 (2009)
- [30] A. Adare *et al.*, arXiv:1501.06197 [nucl-ex].
- [31] J. Adam *et al.* [ALICE Collaboration], arXiv:1506.08804 [nucl-ex].
- [32] B. B. Abelev *et al.* [ALICE Collaboration], Phys. Lett. B **740**, 105 (2015)